

Polarization and Breakdown Analysis of AlGaN Channel HEMTs with AlN Buffer

Godwin Raj^{1*}, Mohan Kumar², Chandan Kumar Sarkar¹

¹Nano Device Simulation Laboratory, Electronics and Telecommunication Engineering Department, Jadavpur University, Kolkata, India

²SKP Engineering College, Tiruvannamalai, India

Email: [*godwinraj123@gmail.com](mailto:godwinraj123@gmail.com)

Received 30 January 2015; accepted 18 August 2015; published 21 August 2015

Copyright © 2015 by authors and Scientific Research Publishing Inc.

This work is licensed under the Creative Commons Attribution International License (CC BY).

<http://creativecommons.org/licenses/by/4.0/>



Open Access

Abstract

We have demonstrated the first carrier density model for AlGaN channel with AlN buffer using spontaneous and piezoelectric polarization comparison with experimental and theoretical results. From the results we proved that the formation of 2DEG in undoped structure relied both on spontaneous and piezoelectric polarization. The electron distribution of Al concentration ($0 < x < 0.5$) was measured for both AlGaN channel and barrier. Barrier thickness assumed between 20 and 25 nm for validating the experimental results. The carrier concentration was observed at the specific interface of the N- and Ga-face by assuming $x_1, x_2 = 0$. The model results are verified with previously reported experimental data.

Keywords

AlGaN Channel, Sheet Carrier Concentration Model, N- and Ga-face, Polarization, High Breakdown, Total Induced Net Interface Polarization

1. Introduction

GaN based HEMTs (High Electron Mobility Transistors) are promising candidates because of their attractive physical properties of higher breakdown electric field, high band gap energy, high frequency operation and high power density. After several attempts, AlGaN/GaN based devices proved its maximum frequency and extreme power density [1] [2]. Compared to Si, the GaN breakdown field is 10 times higher, the band gap is 3 times higher and saturation velocity is 3 times higher. AlN breakdown electric field is 4 times higher, thermal conductance is 1.5 times higher and bandgap is about 2 times higher compared to GaN [3]. Incorporation of Al% in the

*Corresponding author.

channel makes device high breakdown and high temperature operation for next generation high power semiconductor devices. There are few papers reported with AlGa_N as a channel material [4]-[10]. Al_{0.51}Ga_{0.49}N channel and Al_{0.86}Al_{0.14}N barrier proved the maximum breakdown voltage (1800 V) with reduced drain current dispersion. Free standing AlN buffer was used because both substrate materials like Sapphire and 6H-SiC suffered from a lattice mismatch with AlGa_N channel [11]. Recently, Wei *et al.* reported Ultra low DIBL (Drain Induced Barrier Lowering). Coefficient of 6.7 mV/V reported with Al₄₀Ga₆₀N/Al₁₈Ga₈₂N HEMT devices. Also this combination attributed to the poor 2DEG confinement [12]. Optimization of AlGa_N channel HEMT expected to get high performance in the breakdown and power applications. Wurtzite III-V AlGa_N with GaN HEMT device was able to achieve 10¹³/cm² electron density without doping barrier region. Strained AlGa_N/GaN HEMT was also capable of enhancing carrier density in the quantum well because of spontaneous and piezoelectric polarization charge.

2. Device Description

As of previous results AlGa_N-channel HEMT with AlN substrates proved lowest dislocation density of 10⁶/cm² [13]-[15]. In this study, we analyzed the Polarization properties of AlGa_N channel with AlGa_N barrier on AlN buffer and AlN/Sapphire Substrate.

Figure 1 shows the schematic structure of low Al composition channel and barrier with $x < 0.5$. Thickness of AlN buffer layer assumed as per the critical thickness of 1.2 μm. AlGa_N channel placed above the buffer with 600 nm. 25 nm thickness of the AlGa_N barrier placed above the channel. The AlN buffer was used for high quality growth.

In this article we focus on device characterization and polarization of Nface and Ga face AlGa_N/AlGa_N (AlGa_N channel) heterostructures. Formation of 2DEG using spontaneous and piezoelectric polarization for varying mole fraction x_1 and x_2 (N face and Ga face) analyzed using models and experimental comparison. So we concentrate on the polarity of AlGa_N barrier and channel for 2DEG confinement. We assume $x_1 = 0$ for Nface and $x_2 = 0$ for Ga face to verify the results with Ambacher *et al.* [16] the Elastic and elastic constants taken from the same paper.

Even though the thickness AlGa_N barrier assumed as 250 Å the confined charge density is higher as compared to GaN HEMT. Device grown on AlN buffer and sapphire substrate because the lattice mismatch between Substrate and AlGa_N channel as we have seen above. The critical thickness and strain relaxation is the key role for AlGa_N channel HEMT devices because AlGa_N partially relaxed with AlN buffer region [17]. This relaxation assumes in our model as per the experimental results and Al composition up to 0.5 assumed in our model for barrier and channel region. Lattice constant assumed for AlGa_N channel and barrier regions.

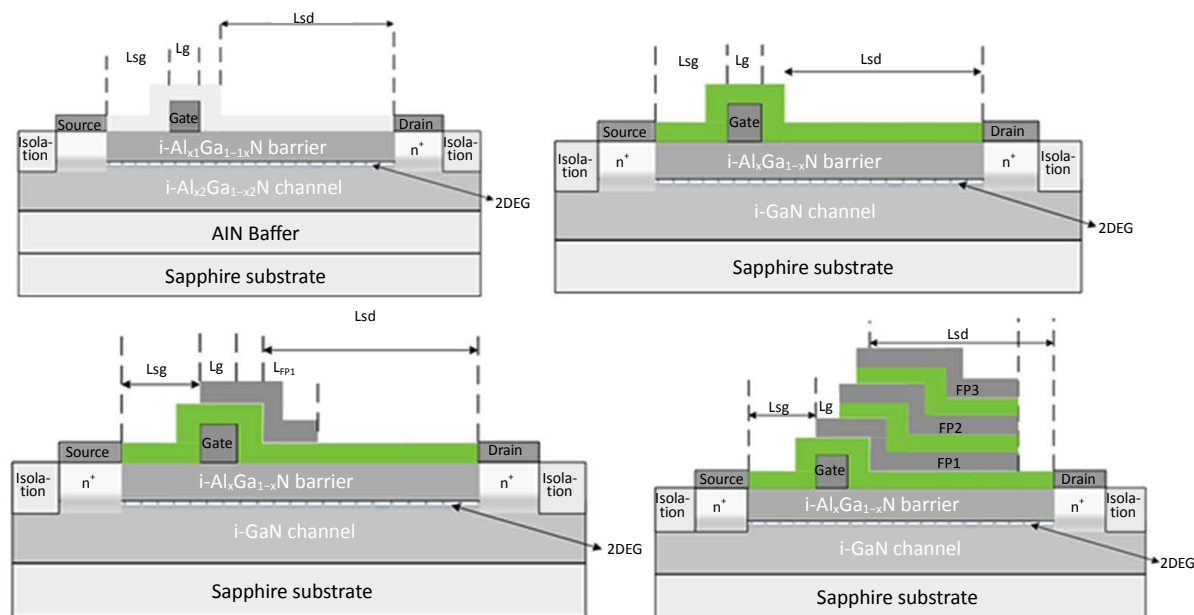


Figure 1. Schematic structure of an AlGa_N/AlGa_N/AlN HEMT with and without field plate.

The spontaneous and piezoelectric polarization induced charge density calculated for Pseudomorphic grown hetero devices not considered separately because we assumed AlGaN partially relaxed with barrier as per the composition and experimental data's. The relaxation rate assumed as per experimental comparison later.

Even unundoped barrier can confine carrier density 2DEG in the channel because of the high structural quality interface between AlGaN channel and buffer region. C-V profile measurement assumed the well known technique for measuring the carrier concentration at room temperature. The model used for C-V measurement is given below [16]

$$N_{c-v} = \frac{C^3}{e\epsilon_0\epsilon} \frac{dV}{dC}, \tag{1}$$

Here C is the capacitance per unit area, V is the applied voltage at the gate to barrier interface, ϵ is the dielectric constant of the material ($\epsilon_0 = 8.854 \times 10^{-14}$ C/V cm; $e = 1.602 \times 10^{-19}$ C).

The main consequences of model and experimental comparison arise

- 1) How the Piezo electric polarization occurs in AlGaN channel and the barrier interface.
- 2) Why the carrier concentration based on the relaxation of these two interfaces.

To answer these questions we should understand the role and physical properties of spontaneous and piezoelectric polarization.

3. Spontaneous and Piezoelectric Polarization

The polarization charge relaxed, tensile strained and compressively strained layer shown in **Figure 2** for Ga, N face heterostructures. In Ga face tensile strained region, spontaneous and piezoelectric polarization assumed to be parallel and compressively strained region, Polarization is antiparallel. This polarization reverses for N face polarization. Here three AlGa N regions assumed with composition of x_1, x_2 and x_3 . For validate our results with Ambacher *et al.* for Ga and N face [16] we assumed x_1 and x_3 to 0 (GaN).

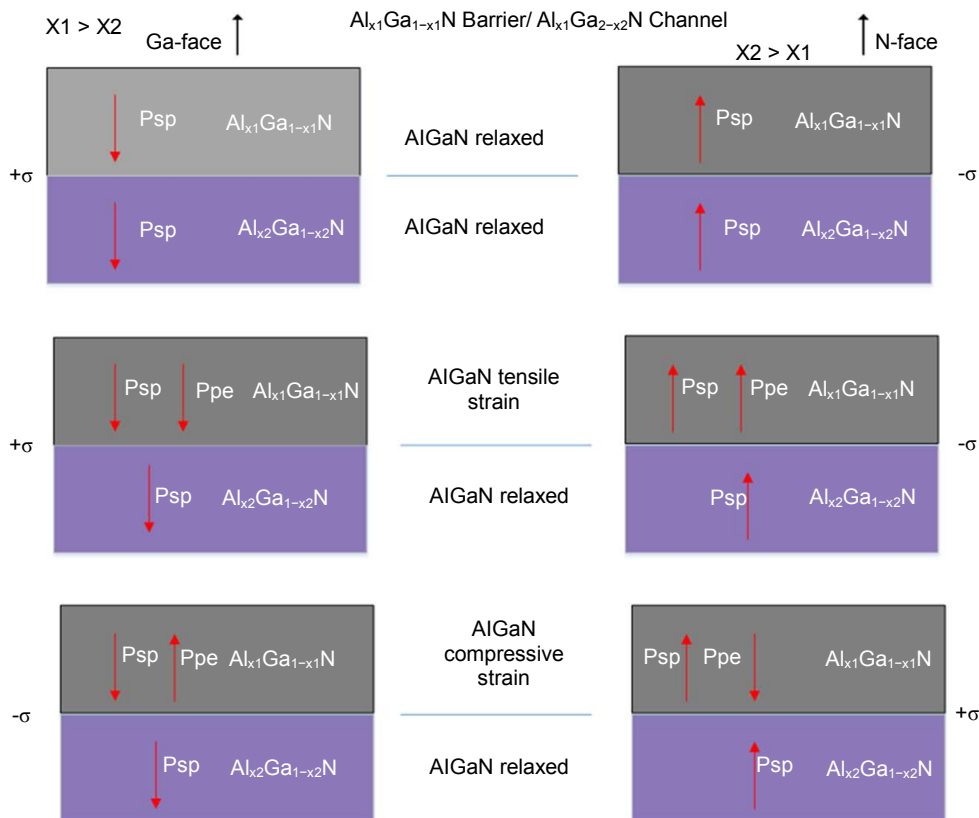


Figure 2. Spontaneous and piezoelectric induced charge in Ga and N face AlGaN/AlGaN heterostructures.

The total confined charge σ_{int} at AlGaN/AlGaN interface is the sum of spontaneous polarization P_{sp} and strain induced piezoelectric polarization at the interface of AlGaN channel. Spontaneous polarization is mainly increased by the Al difference between a barrier and channel region. Spontaneous polarization assumed in [0001] plane. Piezoelectric polarization mainly depends on the strain relaxation occurred between interfaces. It can be modelled by Elastic coefficient e_{31} , e_{33} . e_{15} is sheer strain induced by piezoelectric polarization is not incorporated here. Hexagonal lattice constant of AlGaN/AlGaN is given by

$$P_{PE} = 2 \cdot \left(\left(\frac{a_{\text{AlGaN_ch}}}{a_{\text{AlGaN_br}}} - 0.93 \right) \left[e_{31_br} - \frac{e_{33_br} \cdot c_{13_br}}{c_{33_br}} \right] \right) \quad (2)$$

where c_{33} and c_{11} are the elastic constants. The total polarization induced by piezoelectric polarization at AlGaN/AlGaN interface is given by

$$\begin{cases} c_{13_br} = (5x_1 + 103) \\ c_{33_br} = (-32x_1 + 405) \\ c_{13_ch} = (5x_2 + 103) \\ c_{33_ch} = (-32x_2 + 405) \end{cases} \quad (3)$$

Elastic coefficient parameters for AlGaN channel is given by

$$\begin{cases} e_{31_br} = (-11x_1 - 0.49) \\ e_{33_br} = (0.73x_1 + 0.73) \\ e_{31_ch} = (-11x_2 - 0.49) \\ e_{33_ch} = (0.73x_2 + 0.73) \end{cases} \quad (4)$$

Lattice constant for AlGaN channel and barrier is given by

$$\begin{aligned} a_{\text{AlGaN_br}} &= (3.189 - 0.077x_1)10^{-10} \text{ m} \\ a_{\text{AlGaN_ch}} &= (3.189 - 0.077x_2)10^{-10} \text{ m} \end{aligned} \quad (5)$$

Spontaneous polarization is given by

$$\begin{aligned} P_{sp_AlGaN_br} &= (-0.52x_1 - 0.029) \\ P_{sp_AlGaN_ch} &= (-0.52x_2 - 0.029) \end{aligned} \quad (6)$$

Total polarization induces a charge for N face and Ga face is given by [Figure 3](#) and [Figure 4](#).

Strain induced charge is the main source of carrier concentration in AlGaN/GaN heterostructures. Piezoelectric polarization of AlGaN channel and barrier can be modelled with a single strain relax at the interface. The confined charge density with spontaneous and piezoelectric polarization charge density is given by

$$P_{sp_tot} = [P_{sp_AlGaN_br} - P_{sp_AlGaN_ch}] \quad (7)$$

Piezoelectric polarization uses the elastic parameters from Equations (3) and (4)

$$\begin{aligned} P_{pz_AlGaN_br} &= -2 \cdot (1 - \text{strainrelax}) \cdot \text{strain} \left[e_{31_br} - \frac{e_{33_br} \cdot c_{13_br}}{c_{33_br}} \right] \\ P_{pz_AlGaN_ch} &= -2 \cdot (1 - \text{strainrelax}) \cdot \text{strain} \left[e_{31_ch} - \frac{e_{33_ch} \cdot c_{13_ch}}{c_{33_ch}} \right] \\ P_{pz_tot} &= P_{pz_AlGaN_br} - P_{pz_AlGaN_ch} \\ \sigma(x) &= [P_{sp_tot} + P_{pz_tot}] \end{aligned} \quad (8)$$

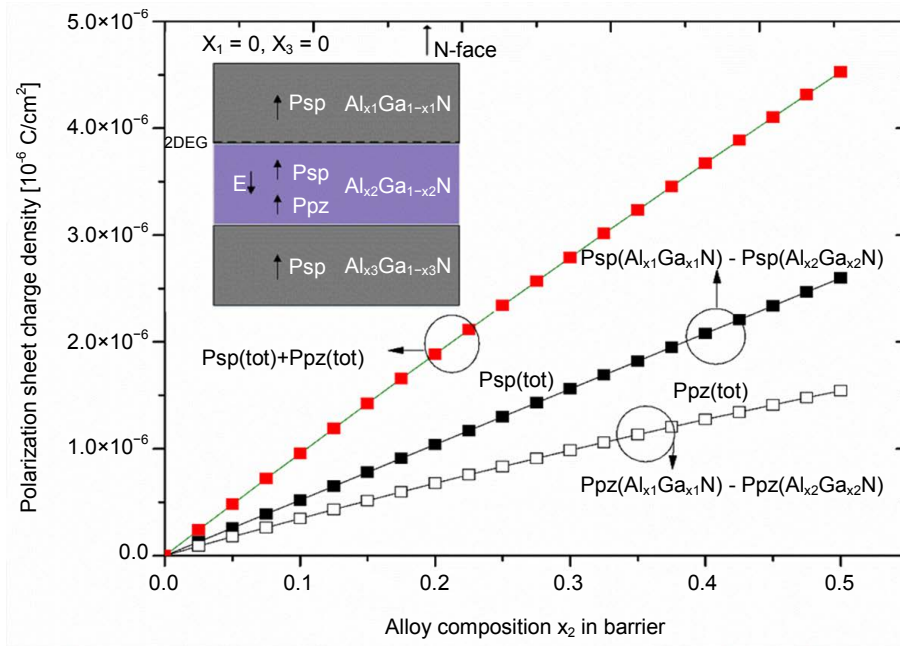


Figure 3. Piezoelectric and spontaneous polarization charge density for various AlGaN barrier alloy compositions for N face $Al_{x_1}Ga_{1-x_1}N/Al_{x_2}Ga_{1-x_2}N/Al_{x_3}Ga_{1-x_3}N$ heterostructures.

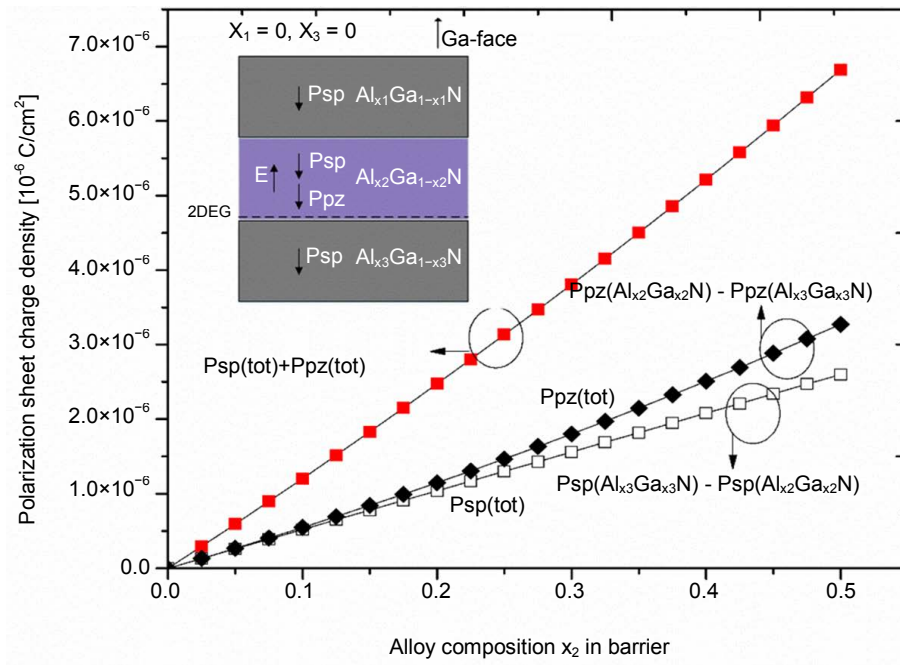


Figure 4. Spontaneous and Piezoelectric polarization charge density for various AlGaN barrier alloy compositions for Ga face $Al_{x_1}Ga_{1-x_1}N/Al_{x_2}Ga_{1-x_2}N/Al_{x_3}Ga_{1-x_3}N$ heterostructures.

4. Relaxation Rate

The degree of relaxation $r(x)$ was calculated by

$$\gamma = \frac{a_AlGaN_ch - a_AlGaN_br}{a_AlGaN_ch^{(0)} - a_AlGaN_br^{(0)}} \tag{9}$$

Here $a_{\text{AlGaN_ch}}^{(0)}$, $a_{\text{AlGaN_br}}^{(0)}$ are the zero strain lattice constant. $a_{\text{AlGaN_ch}}$, $a_{\text{AlGaN_br}}$ are the measured lattice constant parameter [17]. Strain relaxation first observed for 200 - 250 Å°. The degree of relaxation increased by increasing Al composition in the barrier this leads to reduction of piezoelectric polarization. The approximated strain relaxation model for inducing charge given by

$$\gamma = \begin{cases} 0.48 & 0 < x_1 < 0.4 \\ 0.6x_1 + 0.02 & 0.4 < x_1 < 0.53 \end{cases} \quad (10)$$

5. Carrier Concentration Model

An electron from barrier tends to compensate at AlGaN/AlGaN interface for Ga (Al or N face). The confined carrier density for undoped device structure combination is given by [16]

$$n(x) = \frac{\sigma(x)}{e} - \left(\frac{\epsilon_0 \epsilon(x)}{d_{\text{AlGaN}} \cdot e^2} (e\Phi_b(x) + E_f(x) - \Delta E_c) \right) \quad (11)$$

Here $\epsilon(x)$ is the dielectric constant, $e\Phi_b$ is the gateSchottky-barrier height for $\text{Al}_{x_1}\text{Ga}_{1-x_1}\text{N}$ and gate interface,

$$\begin{aligned} \epsilon(x) &= (-0.5x_1) + 9.5; \\ e\Phi_b(x) &= (1.3x_1 + 0.84) \text{ eV}; \end{aligned} \quad (12)$$

Total carrier confined in 2DEG Channel in Ga and N Face calculated using Equation (11) shown in **Figure 5**. Here E_f is the Fermi energy level with respect to the $\text{Al}_{x_2}\text{Ga}_{1-x_2}\text{N}$ channel, e is the charge of the electron, d is the thickness of the barrier.

$$\begin{cases} E_g(\text{AlN}) = 6.13 \text{ eV}; \\ E_g(\text{GaN}) = 3.42 \text{ eV}; \\ E_g(\text{AlGaN_br}) = x_1 E_g(\text{AlN}) + (1-x_1) E_g(\text{GaN}) - x_1(1-x_1) 1.0 \text{ eV}; \\ E_g(\text{AlGaN_ch}) = x_2 E_g(\text{AlN}) + (1-x_2) E_g(\text{GaN}) - x_2(1-x_2) 1.0 \text{ eV}; \\ \Delta E_c = 0.7 [E_g(\text{AlGaN_br}) - E_g(\text{AlGaN_ch})] \text{ eV}; \end{cases} \quad (13)$$

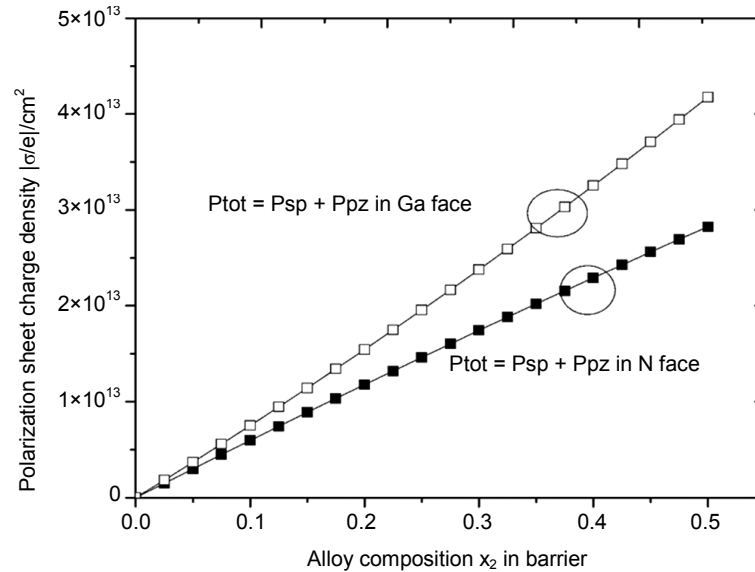


Figure 5. Total polarization charge induced by spontaneous and piezoelectric polarization on Ga and N face.

ΔE_c is the conduction band offset between AlGaN channel and barrier interface.

6. Field Plate Effects and Device Optimization Characteristics

The breakdown characteristics boosted drastically by FP employed over gate electrode towards drain side. Its characterized by electric field profile between gate and drain region. FP length varied systematically by consider specific insulator. Si_3N_4 insulator employed to reduce trap density, reduce leakage and to increase breakdown voltage. In our simulation, 1 μm field plate length assigned. As the field plate length varied, enhancement of breakdown voltage reported. No further breakdown beyond certain field plate length. Its assumed to be an material limit for Field plated analysis.

To enhance further breakdown voltage, GaN Channel replaced by AlGaN Channel material. With this technique, the maximum breakdown voltage of 1750 V Reported for MGFP. However, it should be noted that the peak electric field distributed for higher V_{ds} . But trap density increased between AlGaN and Buffer region. Besides simulation performed for three Field plate devices, results clearly indicates the tradeoff between breakdown voltage and drain current. Drastic enhancement of V_{br} reported in AlGaN Channel HEMT Devices.

7. Results and Discussion

The experimental results and proposed model results show excellent concurrence for predicting sheet carrier concentration characteristics for AlGaN channel for both Ga and N face interfaces with respect to different material compositions.

Figure 6 shows the sheet carrier concentration with barrier thickness. Barrier thickness we assumed from 19 nm to 80 nm. A sheet carrier concentration much reduced because of the less strain relaxes between $\text{Al}_{0.1}\text{Ga}_{0.9}\text{N}/\text{GaN}$ interfaces. Incorporation of low Al about 0.05 in the channel makes less conduction band discontinuity because of less Al difference between the barrier and the channel region. Change in barrier thickness also not affected the channel much because of less Al composition. Our model much consistent with GaN based device also.

Figure 7 shows the variation of sheet carrier concentration n_s with barrier thickness. From the results it clearly evident that AlGaN strained with GaN. As the barrier thickness increases carrier concentration also increases to $1.9 \times 10^{13}/\text{cm}^2$. This variation of barrier thickness increases carrier concentration up to reach its critical level. Interpolation of Al in the channel leads to reduce the carrier density to $1.2 \times 10^{13}/\text{cm}^2$ for the maximum barrier thickness.

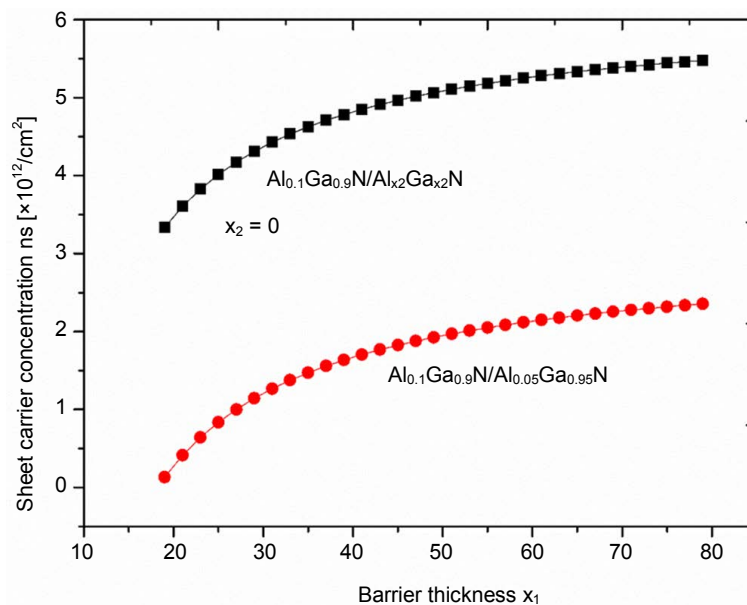


Figure 6. Sheet carrier concentration of less ($x_1 = 0.1$, $x_2 = 0$ and $x_1 = 0.1$, $x_2 = 0.05$) Al composition in the barrier and the channel region with barrier thickness.

Figure 8 shows the partial AlGa_N with GaN. These results are considered with zero strain relax and the carrier concentration assumes to be very high, compared with the low Al composition barrier. Confined well depth increases as the Al composition increases. The variation of sheet carrier concentration taken for GaN channel HEMT. In this fig mole fraction x_2 varied from 0 - 0.3. For high Al difference high sheet charge density expected. Incorporation of Al in the channel makes the growth quality high with AlN buffer. Our model results best match with these results.

Figure 9 shows the incorporation of Al in N face Al_{0.1}Ga_{0.9}N/Al_{0.5}Ga_{0.5}N device. The carrier concentration shows negative carrier density because of N face charge density. Modulus not taken in this plot for N face. Variation of sheet carrier density with barrier considered as x_2 . As AlGa_N channel thickness increases the confined charge shows less negative values.

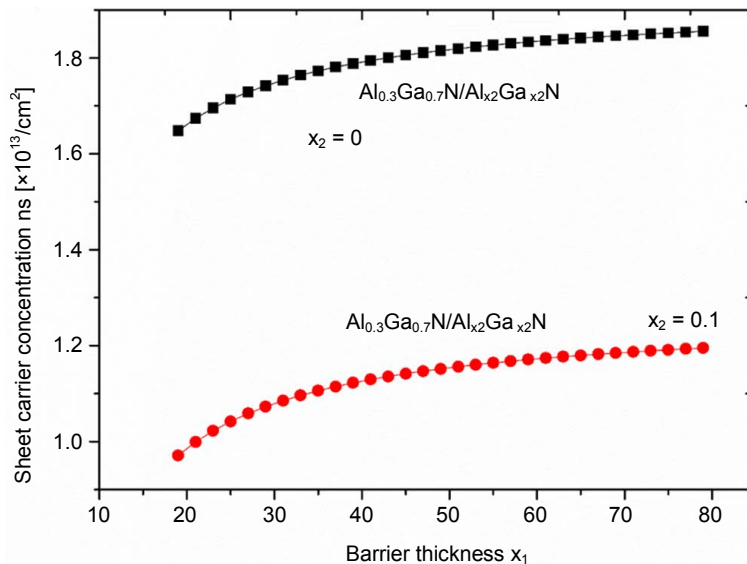


Figure 7. Charge density for moderate Al composition ($x_1 = 0.3$, $x_2 = 0$ and $x_1 = 0.3$ and $x_2 = 0.1$) between barrier and channel with barrier thickness.

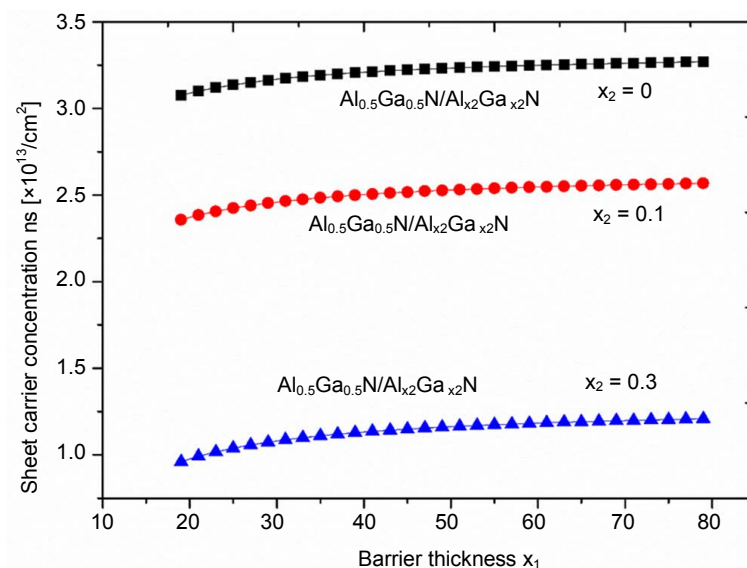


Figure 8. Sheet carrier concentration for High Al composition difference ($x_1 = 0.5$, $x_2 = 0$, $x_1 = 0.5$, $x_2 = 0.1$ and $x_1 = 0.5$, $x_2 = 0.3$) between barrier and channel with barrier thickness.

Figure 10 shows the variation of sheet carrier concentration as the barrier thickness increases. The composition used here for Ga-face HFET is $\text{Al}_{0.5}\text{Ga}_{0.5}\text{N}/\text{Al}_{0.1}\text{Ga}_{0.9}\text{N}$. The Composition shows the clear evidence of incorporation of Al in Ga face heterostructures. These results shows that as the barrier thickness increases confined charge density also increased.

Figure 11 shows the comparison of experimental results published with the proposed model [4]-[10].

Figure 12 and **Figure 13** show the variation of drain current with respect to drain voltage in GaN Channel and $\text{Al}_{0.5}\text{Ga}_{0.5}\text{N}$ channel HEMT. It's verified with GaN buffer, $\text{Al}_{0.1}\text{Ga}_{0.9}\text{N}$ Back Barrier (BB), $\text{Al}_{0.1}\text{Ga}_{0.9}\text{N}$ BB & MGFP1 and $\text{Al}_{0.05}\text{Ga}_{0.95}\text{N}$ BB & $\text{Al}_{0.1}\text{Ga}_{0.9}\text{N}$ BB & MGFP2.

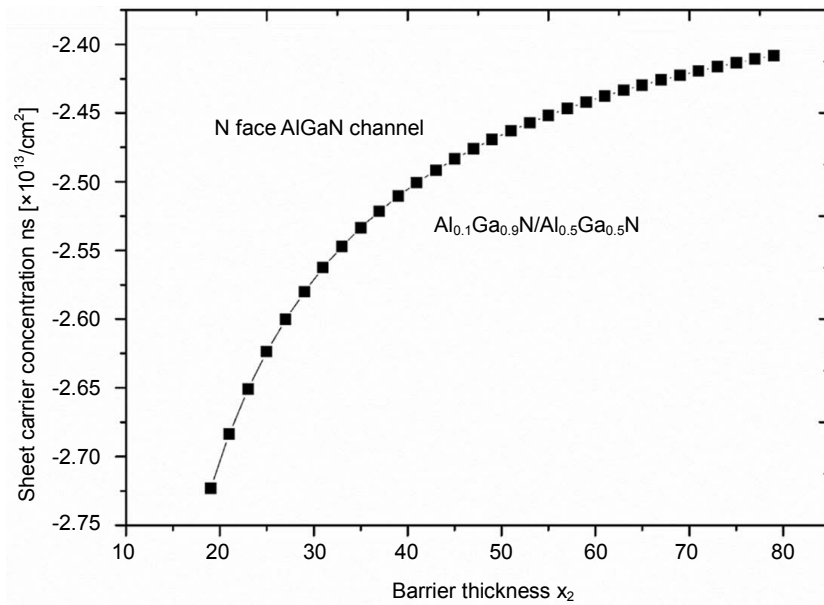


Figure 9. Variation of carrier concentration in the N face AlGaN channel with barrier thickness. Assumed $x_1 = 0.1$ and $x_2 = 0.5$.

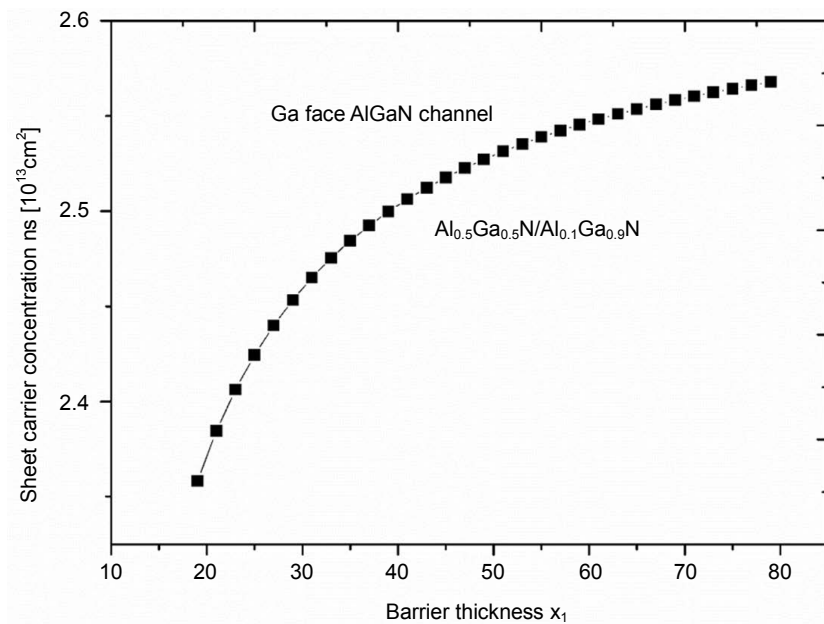


Figure 10. Change of Sheet carrier concentration in Ga face AlGaN channel with barrier thickness. Assumed $x_1 = 0.5$ and $x_2 = 0.1$.

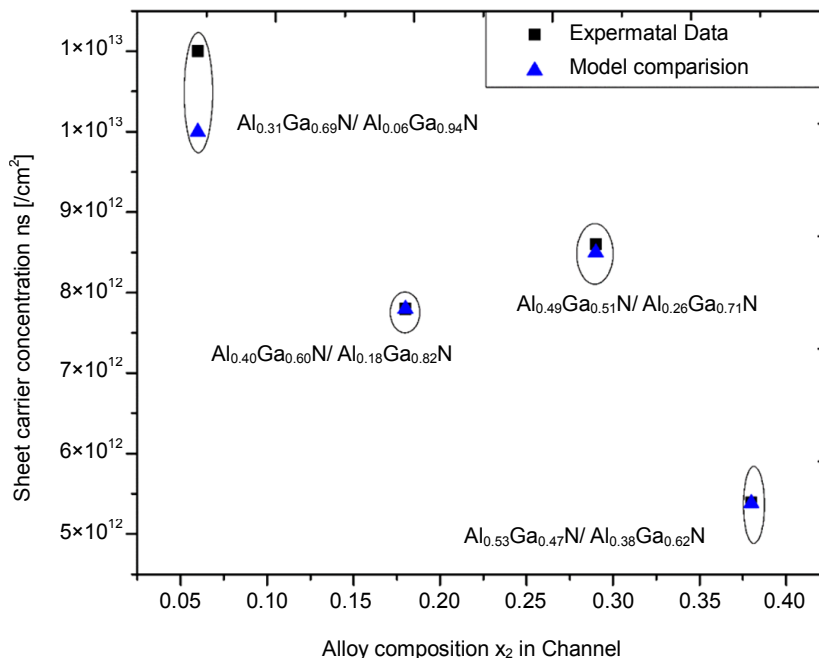


Figure 11. Experimental verification of reported AlGa_N channel results with proposed sheet carrier density model [10].

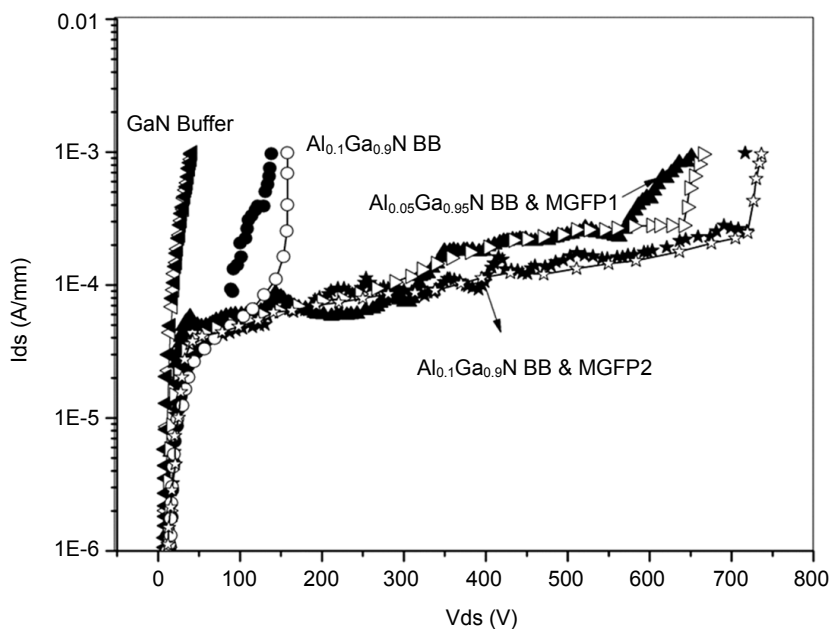


Figure 12. Variation of OFF state drain voltage with drain current. Filled box represents Experimental and empty box represents Simulation validated data.

8. Conclusion

We have analyzed the formation of 2DEG charge density for various alloy compositions in AlGa_N barrier and channel interface regions. The above results were analyzed for both Ga and N face interfaces. Polarization charge density in the AlGa_N channel from low to high Al interpolation was analyzed in detail. From the results, it shows that calculated 2DEG carrier concentration exhibits good agreement with experiment reported values. Incorporation of strain relaxation is essential in AlGa_N channel because of AlN buffer. From the relaxation model,

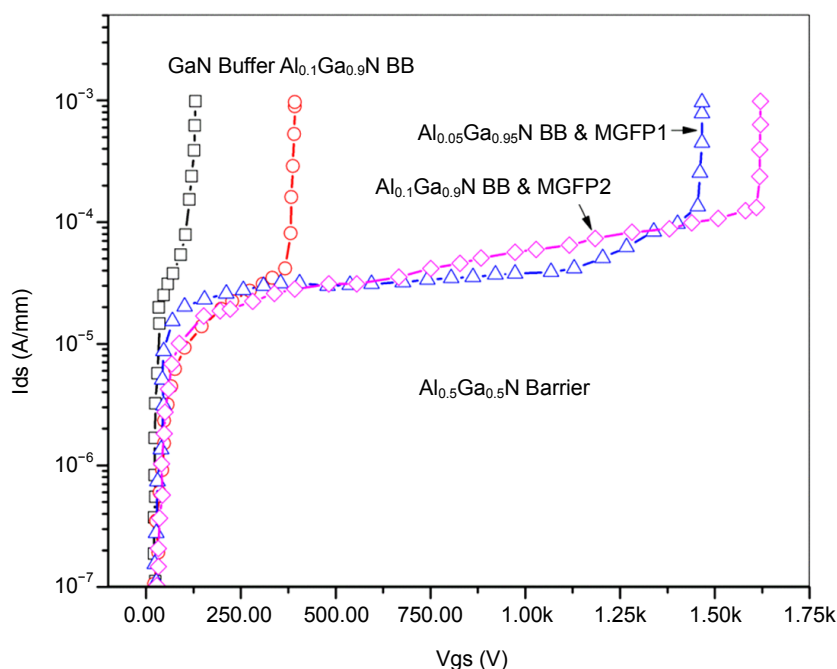


Figure 13. Enhancement of OFF State breakdown voltage with drain current for Al-GaN channel HEMTs.

adding Al composition in Channel leads to create strain relaxation in barrier. Our theoretical results prove that incorporation of Al makes device possible for future high power and high frequency application.

Acknowledgements

The authors thank the Council of Scientific and Industrial Research for financially supporting this research.

References

- [1] Chung, J.W., Hoke, W.E., Chumbes, E.M. and Palacios, T. (2010) AlGaIn/GaN HEMT With 300-GHz f_{max} . *IEEE Electron Device Letters*, **31**, 195-197. <http://dx.doi.org/10.1109/LED.2009.2038935>
- [2] Wu, Y.F., Saxler, A., Moore, M., Smith, R.P., Sheppard, S., Chavarkar, P.M., Wisleder, T., Mishra, U.K. and Parikh, P. (2004) 30-W/mm GaN HEMTs by Field Plate Optimization. *IEEE Electron Device Letters*, **25**, 117-119. <http://dx.doi.org/10.1109/LED.2003.822667>
- [3] Hashimoto, S., Akita, K., Tanabe, T., Nakahata, H., Takeda, K. and Amano, H. (2010) Epitaxial Layers of AlGaIn Channel HEMT on AlN Substrates. *SEI Technical Review*, **71**, 83.
- [4] Raman, A., Dasgupta, S., Rajan, S., Speck, J.S. and Mishra, U.K. (2008) AlGaIn Channel High Electron Mobility Transistors: Device Performance and Power-Switching Figure of Merit. *Japanese Journal of Applied Physics*, **47**, 3359. <http://dx.doi.org/10.1143/JJAP.47.3359>
- [5] Nanjo, T., Takeuchi, M., Suita, M., Abe, Y., Oishi, T., Tokuda, Y. and Aoyagi, Y. (2008) First Operation of AlGaIn Channel High Electron Mobility Transistors. *Applied Physics Express*, **1**, Article ID: 011101. <http://dx.doi.org/10.1143/APEX.1.011101>
- [6] Nanjo, T., Takeuchi, M., Suita, M., Abe, Y., Oishi, T., Abe, Y., Tokuda, Y. and Aoyagi, Y. (2008) Remarkable Breakdown Voltage Enhancement in AlGaIn Channel high Electron Mobility Transistors. *Applied Physics Letters*, **92**, Article ID: 263502. <http://dx.doi.org/10.1063/1.2949087>
- [7] Nanjo, T., Suita, M., Oishi, T., Abe, Y., Yagyu, E. and Tokuda, Y. (2009) Comparison of the Characteristics of the AlGaIn Channel HEMTs Formed on SiC and Sapphire Substrates. *Electronics Letters*, **45**, 424. <http://dx.doi.org/10.1049/el.2009.0129>
- [8] Jeon, C.M. and (2004) The Improvement of DC Performance in AlGaInGaN HEMTs With Isoelectronic Al-Doped Channels. *IEEE Electron Device Letters*, **25**, 120-122. <http://dx.doi.org/10.1109/LED.2004.824246>
- [9] Liu, J., Zhou, Y., Chu, R., Cai, Y., Chen, K.J. and Lau, K.M. (2004) Al_{0.3}Ga_{0.7}N/Al_{0.05}Ga_{0.95}N/GaN Compos-

- ite-Channel HEMTs with Enhanced Linearity. *International Electron Devices Meeting (IEDM)*, 811.
- [10] Liu, J., Zhou, Y., Chu, R., Cai, Y., Chen, K.J. and Lau, K.M. (2005) Highly Linear $\text{Al}_{0.3}\text{Ga}_{0.7}\text{N}-\text{Al}_{0.05}\text{Ga}_{0.95}\text{N}-\text{GaN}$ Composite-Channel HEMTs. *IEEE Electron Device Letters*, **26**, 145-147. <http://dx.doi.org/10.1109/LED.2005.843218>
- [11] Bajaj, S., Hung, T.-H., Akyol, F., Nath, D. and Rajan, S. (2014) Modeling of High Composition AlGa_xN Channel High Electron Mobility Transistors with Large Threshold Voltage. *Applied Physics Letters*, **105**, Article ID: 263503. <http://dx.doi.org/10.1063/1.4905323>
- [12] Ha, W., Zhang, J.-C., Zhao, S.-L., Ge, S.-S., Wen, H.-J., Zhang, C.-F., Ma, X.-H. and Hao, Y. (2013) AlGa_xN Channel High Electron Mobility Transistors with Ultra-Low Drain-Induced-Barrier-Lowering Coefficient. *Chinese Physics Letters*, **30**, Article ID: 127201. <http://dx.doi.org/10.1088/0256-307X/30/12/127201>
- [13] Hashimoto, S., Akita, K., Tanabe, T., Nakahata, H., Takeda, K. and Amano, H. (2010) Sublimation Growth of Nonpolar AlN Single Crystals and Defect Characterization. *Physica Status Solidi (C)*, **7**, 1767-1769. <http://dx.doi.org/10.1002/pssc.200983590>
- [14] Hatano, M., Kunishio, N., Chikaoka, H., Yamazaki, J., Makhzani, Z.B., Yafune, N., Sakuno, K., Hashimoto, S., Akita, K., Yamamoto, Y. and Kuzuhara, M. (2010) Comparative High-Temperature DC Characterization of HEMTs with GaN and AlGa_xN Channel Layers. *CS MANTECH Conference*, 17-20 May 2010, Portland.
- [15] Tokuda, H., Hatano, M., Yafune, N., Hashimoto, S., Akita, K., Yamamoto, Y. and Kuzuhara, M. (2010) High Al Composition AlGa_xN-Channel High-Electron-Mobility Transistor on AlN Substrate. *Applied Physics Express*, **3**, Article ID: 121003. <http://dx.doi.org/10.1143/APEX.3.121003>
- [16] Ambacher, O., Smart, J., Shealy, J.R., Weimann, N.G., Chu, K., Murphy, M., Schaff, W.J. and Eastman, L.F. (1999) Two-Dimensional Electron Gases Induced by Spontaneous and Piezoelectric Polarization Charges in N- and Ga-Face AlGa_xN/GaN Heterostructures. *Journal of Applied Physics*, **85**, 3222. <http://dx.doi.org/10.1063/1.369664>
- [17] Asai, T., Nagata, K., Mori, T., Nagamatsu, K., Iwaya, M., Kamiyama, S., Amano, H. and Akasaki, I. (2009) Relaxation and Recovery Processes of Al_xGa_{1-x}N Grown on AlN Underlying Layer. *Journal of Crystal Growth*, **311**, 2850-2852. <http://dx.doi.org/10.1016/j.jcrysgro.2009.01.028>